$Yb_{14}ZnSb_{11}$: Charge Balance in Zintl Compounds as a Route to Intermediate Yb Valence

I. R. Fisher, S. L. Bud'ko, C. Song, and P. C. Canfield
Ames Laboratory and Department of Physics and Astronomy, Iowa State University, Ames, Iowa 50011

T. C. Ozawa and S. M. Kauzlarich
Department of Chemistry, University of California, One Shields Avenue, Davis, California 95616
(Received 29 February 2000)

The results of thermodynamic, transport, and x-ray diffraction measurements of single crystals of the new compound $Yb_{14}ZnSb_{11}$ are presented. These data indicate an intermediate Yb valence scenario, with a spin fluctuation temperature of approximately 85 K. The compound is weakly metallic and is isostructural with the charge-balanced Zintl compound $Yb_{14}AlSb_{11}$. The intermediate Yb valence can be qualitatively accounted for by considering the charge counting arguments of the nonmetallic parent, and charge balance in Zintl-related materials appears to be a viable route to designing other compounds with intermediate valence constituents.

PACS numbers: 75.20.Hr, 75.30.Mb

Zintl phases make up a class of materials that are electronically positioned between intermetallic compounds and insulating valence compounds. They are typically characterized by a small semiconducting gap and charge counting arguments can be used as a mechanism to stabilize certain crystal structures [1]. The Zintl concept is therefore complementary to the arguments of Hume-Rothery. Both systems try to account for observed crystal structures in terms of the electronic properties, albeit one argument being in terms of predominantly ionic bonding and the other in terms of valence electron concentration. In this particular case, we have taken the nonmagnetic nonmetallic Zintl compound $Yb_{14}AlSb_{11}$ for which all Yb are divalent and tuned the electronic properties by substituting divalent Zn for trivalent Al. The new compound $Yb_{14}ZnSb_{11}$ has the same structure, appears to be more metallic in character and demonstrates an intermediate Yb valence. This compound extends our understanding of ytterbium pnictide compounds and indicates a possible route for the design of other intermediate valence systems.

Zintl-related compounds might at first sight appear unlikely to yield unusual ambivalent behavior, typically having a low carrier density. However, low carrier concentration compounds have already been discovered for which Yb hybridization effects are thought to be very significant at low temperatures. For instance, YbBiPt is also closely related to a series of semiconducting or semimetallic materials [2,3], and has an exceptionally large linear-in-temperature component of the heat capacity of $\gamma = 8\ \mathrm{J/mol\,K^2}$ [2,4]. Other ytterbium pnictide compounds show a range of magnetic properties [5]. In particular, the Yb_4Pn_3 (Pn = As, Sb, Bi) series of compounds have a relatively low carrier concentration and exhibit a range of valence fluctuation as the relative position of the $4f$ level shifts with respect to the Fermi energy for the different size pnictogen [6–8].

The architypical member of the "14-1-11" family is the Zintl compound $Ca_{14}AlSb_{11}$ [9], crystallizing in the tetragonal system $I4_1/acd$. This structure is apparently charge balanced, consisting of 14 A^{2+} ions, 4 Pn^{3-} ions, a hypervalent linear Pn_3^{7-} unit, and a MPn_4^{9-} tetrahedron, where A is typically a group II element, Pn is a pnictogen, and M is typically a trivalent metal [10]. There are 8 such formula units per unit cell, with 4 inequivalent A sites having multiplicities of 2, 4, 4, and 4. The M ions are well separated, with an approximate M-M distance of 10 Å. The recent discovery of other 14-1-11 compounds based on $A = Yb^{2+}$ or Eu^{2+}, and also $M = Mn$ [11–13] has presented a valuable opportunity for the investigation of several unusual magnetic and electronic effects. We recall that Yb^{2+} has a filled $4f$ electron shell and as such is nonmagnetic, whereas Eu^{2+} has a half filled f shell and possesses a large magnetic moment. For instance, $Eu_{14}MnSb_{11}$ appears to be an intermetallic collosal magnetoresistive material, having a metal-insulator transition associated with a ferromagnetic phase transition at $T_C = 92$ K [14]. In addition, the more metallic compound $Yb_{14}MnSb_{11}$ is a very clear example of what might be dubbed a dilute transition metal compound, in which all of the magnetic properties arise from well-separated Mn^{3+} ions which appear to be acting as local moments with the full spin-only Hund's rule value, and which order ferromagnetically at 52 K [15].

Until now, Zn-containing 14-1-11 compounds such as $Ca_{14}ZnSb_{11+\Delta}$ have invariably contained some additional interstitial Sb ($\Delta \sim 0.2$–0.4, depending slightly on the alkaline earth element). The element Zn always forms a divalent ion due to the stability of the full $3d$ shell, and the additional interstitial Sb acts to formally balance the charges and maintain the semiconducting properties [10]. Following the Zintl argument, it appears that charge balance is required to stabilize the 14-1-11 structure. Significantly, the new compound $Yb_{14}ZnSb_{11}$ has the architypical 14-1-11 structure, but in contrast to the alkaline earth Zn-containing 14-1-11 compounds, refinement of single-crystal x-ray diffraction data reveals a stoichiometric

 0031-9007/00/85(5)/1120(4)$15.00

compound within standard deviations, with no evidence for any interstitial inclusions.

Single crystals of $Yb_{14}ZnSb_{11}$ were grown from a Sn flux, as described previously for $Yb_{14}MnSb_{11}$ [15]. The multifaceted morphology of the crystals did not suggest any obvious crystallographic orientation, and Laue x-ray diffraction patterns were necessary to align the crystals for susceptibility measurements in high symmetry directions. Temperature-dependent dc susceptibility measurements from 1.8 to 350 K were made using a commercial Quantum Design MPMS5 SQUID magnetometer, in an applied field of 1 kOe. Bars were polished in arbitrary orientations for resistivity measurements, which were made using a standard 4-probe technique, with an ac bridge operating at 16 Hz and with typical current densities of 0.05 $A\,cm^{-2}$. Heat capacity measurements were made for a relatively large single crystal with a flat surface polished for improved thermal contact. A Quantum Design PPMS system was used for these measurements, utilizing a relaxation technique with typical temperature changes of approximately 30 mK below 20 K. Single-crystal x-ray diffraction data were acquired using a SMART 1000 Bruker AXS CCD diffractometer. X rays were generated at 50 kV and 40 mA using a Mo target with a graphite monochromator, and the samples were mounted in a cold nitrogen gas stream at 90 K. Lattice parameters of $Yb_{14}ZnSb_{11}$ are shown in Table I compared with those of the related compounds $Yb_{14}AlSb_{11}$ and $Yb_{14}MnSb_{11}$ grown by the same technique and measured on the same diffractometer.

The longitudinal dc susceptibility of $Yb_{14}ZnSb_{11}$ is shown in Fig. 1 for applied fields in the [100], [110], and [001] directions (χ_{100}, χ_{110}, χ_{001}, respectively). There is a modest anisotropy in the susceptibility, with an easy axis closer to [100]. For temperatures above approximately 150 K, the susceptibility follows a Curie-Weiss temperature dependence, with Curie constants $C = (4.63, 4.13, \text{and } 5.68) \pm 0.04 \times 10^{-4}$ emu K/g and Weiss constants $\theta = (-223, -294, \text{and } -474) \pm 10$ K for H parallel to [100], [110], and [001] respectively. These Weiss constants indicate predominantly antiferromagnetic interactions, although there is no evidence of such a ground state or even a phase transition to our lowest temperatures. Estimating the polycrystalline average susceptibility by $(2\chi_{100} + \chi_{001})/3$, we find an effective moment of $3.8 \pm 0.1\mu_B$ per formula unit in this temperature range, and an average Weiss temperature of -273 ± 10 K. As can be seen from Fig. 1(b), the estimate of the effective moment is not particularly sensitive to how the polycrystalline average is calculated. There is a broad maximum in the susceptibility at a temperature $T^* \sim 85$ K, the susceptibility falling with decreasing temperature below this. This maximum also shows up clearly in the polycrystalline average of the data, and as such is unlikely to be due to crystalline electric field (CEF) effects. The broad maximum at T^* and the high-temperature effective moment are robust sample-independent features which we believe to be intrinsic to $Yb_{14}ZnSb_{11}$. Below approximately 20 K, the susceptibility again increases with decreasing temperature, this effect being somewhat sample-dependent. We ascribe the low-temperature upturn in the susceptibility to varying small amounts of free Yb^{3+} impurities. The Curie constant associated with this upturn can be accounted for by one Yb^{3+} per approximately 160 formula units and the saturated moment observed at low temperatures in high magnetic fields is entirely consistent with this estimate. These magnetic impurites may be associated with small regions of flux inclusions in the crystals, or may be distributed more evenly through the crystal matrix. In the

TABLE I. Lattice parameters of $Yb_{14}MSb_{11}$, for M = Al, Mn, and Zn, as determined by single-crystal x-ray diffraction:

	a (Å)	c (Å)	c/a	V (Å^3)
$Yb_{14}AlSb_{11}$	16.561(2)	22.102(3)	1.3346(2)	6063.5(1.8)
$Yb_{14}MnSb_{11}$	16.591(2)	21.920(3)	1.3212(2)	6033.6(1.2)
$Yb_{14}ZnSb_{11}$	16.562(3)	21.859(2)	1.3198(3)	5995.9(1.6)

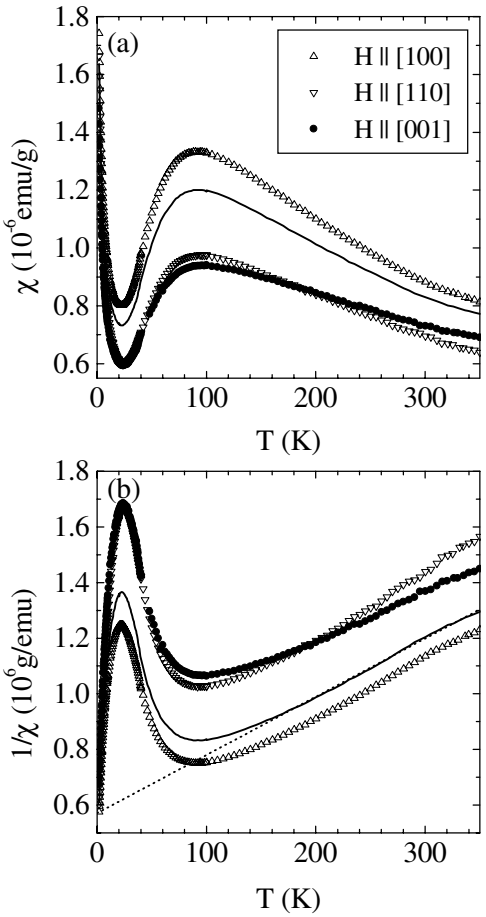

FIG. 1. (a) Susceptibility and (b) inverse susceptibility of $Yb_{14}ZnSb_{11}$ as a function of temperature. Field orientation as shown in legend. Solid line indicates polycrystalline average, as defined in main text. Dashed line in lower panel indicates linear fit to polycrystalline average from 150 to 350 K, with fit parameters given in main text.

nonmagnetic analog $Yb_{14}AlSb_{11}$, similar Yb^{3+} impurity levels are observed, with no associated Kondo behavior down to our base temperature of 1.8 K.

The electrical resistivity of $Yb_{14}ZnSb_{11}$ and $Yb_{14}MnSb_{11}$ is shown in Fig. 2. The rather large values of the room temperature resistivity (around 1 mΩ cm) are consistent with a low carrier density scenario, although Hall measurements are necessary to confirm this statement. Below $T^* \sim 85$ K, as defined from the maximum in the susceptibility, there is a moderately rapid downturn in the resistivity of $Yb_{14}ZnSb_{11}$ with decreasing temperature, culminating in a temperature-independent low-temperature value of approximately 80 $\mu\Omega$ cm. The residual resistance ratio is 13, comparable to that of $Yb_{14}MnSb_{11}$ [15]. While there is a sharp drop in the resistivity of $Yb_{14}MnSb_{11}$ at $T_C = 52$ K due to the loss of spin disorder scattering, the drop in the resistivity of $Yb_{14}ZnSb_{11}$ around $T^* \sim 85$ K is in comparison a much broader feature, consistent with a crossover with this energy scale rather than a phase transition at a specific temperature.

The resistivity of $Yb_{14}AlSb_{11}$ is typical of many Zintl materials [10], and is shown in the inset to Fig. 2. A plot of $\ln\rho$ vs $1/T$ for these data has a slope of approximately 4 K for $T \ll 20$ K, indicating that this material is a small gap semiconductor or a semimetal, in keeping with our observation of a diamagnetic susceptibility for this compound and in contrast to the more metallic behavior of $Yb_{14}ZnSb_{11}$ and $Yb_{14}MnSb_{11}$.

Heat capacity data for $Yb_{14}ZnSb_{11}$ are compared to those of $Yb_{14}AlSb_{11}$ in Fig. 3 (and inset). As can be seen, there is only a modest difference in the heat capacity of the two compounds, and one would hardly describe $Yb_{14}ZnSb_{11}$ as "heavy". A linear extrapolation of C_p/T versus T^2 gives approximate zero-temperature estimates of the linear term in the heat capacity $\gamma = 80$ and 20 mJ/mol K^2 for $Yb_{14}ZnSb_{11}$ and $Yb_{14}AlSb_{11}$, respectively, where one mole refers to one formula unit. Each formula unit contains 26 atoms, probably accounting for the relatively large values of γ measured for $Yb_{14}AlSb_{11}$.

To account for the observed magnetic properties of $Yb_{14}ZnSb_{11}$, we recall that the Hund's rule value for the effective moment of Yb^{3+} is $4.5\mu_B$. Hence, if the Yb site with minimum multiplicity (that is 2) were occupied by Yb^{3+} and the other 3 sites with nonmagnetic Yb^{2+} we would expect to observe an effective moment of $9\mu_B$ per formula unit. That we observe only $3.8\mu_B$ is strong evidence of a homogenous mixed valence (or intermediate valence) scenario, although it remains to be determined by how many of the four different Yb sites this intermediate valence is shared. The lattice parameters of $Yb_{14}ZnSb_{11}$ shown in Table I are certainly not in disagreement with the presence of Yb^{3+} ions (smaller than Yb^{2+}), the cell volume being smaller than that of $Yb_{14}MnSb_{11}$ or $Yb_{14}AlSb_{11}$ which contain only Yb^{2+}. However, it must be remembered the metallic covalency of $Yb_{14}ZnSb_{11}$ will also be acting to contract the lattice in addition to the fraction of smaller Yb^{3+}, and so this evidence is not wholly conclusive of an intermediate valence state, nor is it contradictory.

In an intermediate valence scenario, the temperature T^* can be associated with a spin-fluctuation temperature, below which the Yb^{3+} moments are progressively screened by the conduction electrons. The actual characteristic temperature can be somewhat higher than T^* and may be extracted following Rajan's calculations [16], as done for instance for $YbAgCu_4$ [17]. In this particular case, the relatively large concentration of Yb^{3+} impurities make

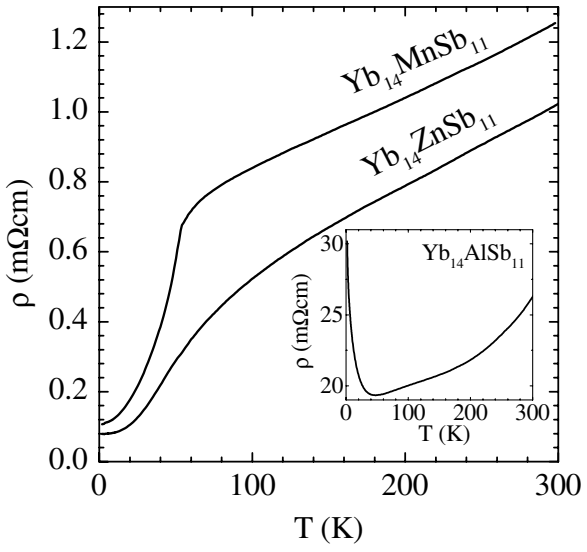

FIG. 2. Electrical resistivity of $Yb_{14}ZnSb_{11}$, $Yb_{14}MnSb_{11}$, and $Yb_{14}AlSb_{11}$ (inset). That of $Yb_{14}MnSb_{11}$ is measured for a current flowing in a direction perpendicular to the c axis, while the others were measured for an arbitrary current orientation with respect to crystal axes.

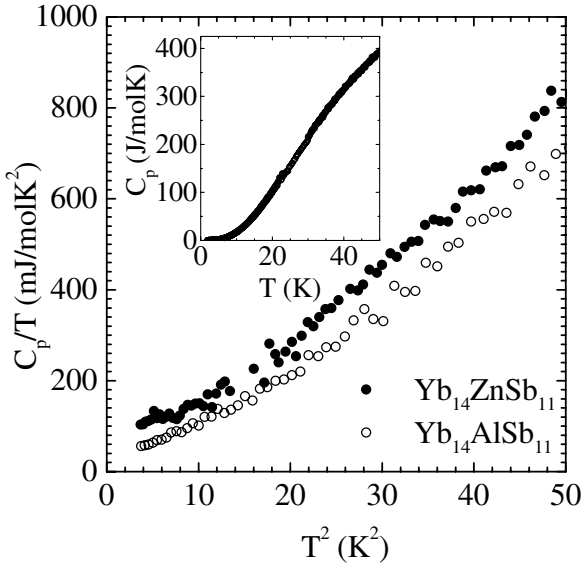

FIG. 3. Heat capacity of $Yb_{14}ZnSb_{11}$ (solid symbols) and $Yb_{14}AlSb_{11}$ (open symbols). Main panel shows C_p/T versus T^2 for temperatures below 7 K. Inset shows C_p as a function of T up to 50 K: on this scale the data for $Yb_{14}ZnSb_{11}$ and $Yb_{14}AlSb_{11}$ are indistinguishable.

estimates of the intrinsic zero-temperature susceptibility difficult and application of the model somewhat impractical. The progressive Kondo screening of the Yb moments as the temperature decreases below T^* results in a decrease in the electrical resistivity, as observed, in addition to an increase in the electronic contribution to the heat capacity. For some intermediate Yb valence compounds, this Kondo screening can contribute rather large values of γ [18]. In this case, the low effective moment per formula unit and the relatively high value of T^* both imply a somewhat smaller contribution to γ, and it is not surprising that we observe only a modest difference between the heat capacity of $Yb_{14}ZnSb_{11}$ and $Yb_{14}AlSb_{11}$. In comparison, Yb_4Sb_3 has a broad peak in the susceptibility at 230 K [6], and a γ value of approximately 50 $mJ/mol\,K^2$ [7].

With such a low γ and relatively high T^*, it can be asked why is $Yb_{14}ZnSb_{11}$ of specific import or interest? The answer lies in the question, why does this material show an intermediate Yb valence? The 14-1-11 crystal structure has already demonstrated its Zintl nature in its reluctance to deviate from a charge-balanced scenario, choosing to accommodate additional interstitial antimony in Zn-containing alkaline earth compounds like $Ca_{14}ZnSb_{11+\Delta}$ rather than adopt a more metallic nature. With the minimum A-site multiplicity being 2, taking on a formal intermediate Yb valence in $Yb_{14}ZnSb_{11}$ while maintaining the correct stoichiometry is potentially another way to balance the charge on substituting Zn for Al. Certainly this was not an option for devoutly divalent A-site species such as the alkaline earths. However, although the charge counting arguments of the Zintl concept have been used to understand the structure and bonding of a wide variety of crystal structures, including other members of the 14-1-11 family, the concept is overly simplistic and in some cases probably incorrect. With such a complex crystal structure, it is difficult to be sure of the origin of the differences in the physical properties of $Yb_{14}ZnSb_{11}$ and $Yb_{14}AlSb_{11}$. However, it is likely most appropriate to think in terms of a band argument, whereby the Fermi level changes as we substitute divalent Zn for trivalent Al, resulting in the observed albeit poor metallic conductivity. Although Zn^{2+} is a larger ion than Al^{3+}, the metallic covalency somewhat contracts the lattice of $Yb_{14}ZnSb_{11}$ with respect to the Zintl analog, which may cause the Fermi energy to partially cross the Yb $4f$ levels. Pressure-dependent measurements of the susceptibility of $Yb_{14}AlSb_{11}$ may help to clarify this and indicate if there are any other more subtle changes that the Zn substitution has on the Yb hybridization. The use of chemical pressure to tune Yb hybridization by squeezing from Yb^{2+} towards a Yb^{3+} state is not unusual. However, in this case it appears that the origin of the chemical pressure is primarily coming from a change from semiconducting to metallic behavior. It can be envisaged that this behavior might be reproduced by tuning the charge balance in other Zintl compounds containing divalent Yb, and as such this appears to be a viable route for the design of other intermediate valence systems, potentially with much larger values of γ.

In conclusion, we have synthesized the new compound $Yb_{14}ZnSb_{11}$, and have presented strong evidence that this is an intermediate Yb valence compound. The intermediate Yb valence can be qualitatively accounted for by considering the Zintl charge counting arguments of the nonmetallic parent $Yb_{14}AlSb_{11}$, and it appears that Zintl-related materials may be a viable route to designing other compounds with intermediate valence constituents. For instance, such behavior might also be seen in the as yet unsynthesized compound $Eu_{14}ZnSb_{11}$. In this case, the presence of a small amount of Eu^{3+} would presumably weaken the magnetic properties, possibly suppressing any eventual magnetic ordering temperature.

We are grateful to N. Anderson, Jr., N. Kelso, and M. Foley for help in sample preparation, J. Schmalian for consistently useful and enjoyable discussions, and M. M. Olmstead for assistance in single-crystal x-ray diffraction work. T. C. O. and S. M. K. were supported by the NSF (DMR-9803074). The Bruker SMART 1000 diffractometer was funded in part by NSF Instrumentation Grant No. CHE-9808259. Ames Laboratory is operated for the U.S. Department of Energy under Contract No. W-7405-ENG-82. This work was supported by the Director for Energy Research, Office of Basic Energy Sciences.

[1] G. J. Miller, in *Chemistry, Structure and Bonding of Zintl Phases and Ions*, edited byS. M. Kauzlarich (VCH, New York, 1996), p. 1.
[2] P. C. Canfield *et al.,* J. Appl. Phys. **70**, 5800 (1991).
[3] D. T. Morelli, P. C. Canfield, and P. Drymiotis, Phys. Rev. B **53**, 12–896 (1996).
[4] Z. Fisk *et al.,* Phys. Rev. Lett. **67**, 3310 (1991).
[5] F. Hulliger, in *Handbook of the Physics and Chemistry of Rare Earths*, edited byK. A. Gschneidner, Jr. and L. Eyring (North-Holland, Amsterdam, 1979), p. 153.
[6] A. Ochiai *et al.,* J. Magn. Magn. Mater. **47–48**, 570 (1985).
[7] A. Ochiai *et al.,* J. Magn. Magn. Mater. **140–144**, 1249 (1995).
[8] V. N. Antonov *et al.,* Phys. Rev. B **58**, 9752 (1998).
[9] G. Cordier, H. Schafer, and M. Stelter, Z. Anorg. Allg. Chem. **519**, 183 (1984).
[10] S. M. Kauzlarich, in *Chemistry, Structure and Bonding of Zintl Phases and Ions*, S. M. Kauzlarich (VCH, New York, 1996), p. 245.
[11] A. Rehr and S. M. Kauzlarich, J. Alloys Compd. **207–208**, 424 (1994).
[12] J. Y. Chan *et al.,* Chem. Mater. **10**, 3583 (1998).
[13] J. Y. Chan *et al.,* Phys. Rev. B **57**, 8103 (1998).
[14] J. Y. Chan *et al.,* Chem. Mater. **9**, 3132 (1997).
[15] I. R. Fisher *et al.,* Phys. Rev. B **59**, 13 829 (1999).
[16] V. T. Rajan, Phys. Rev. Lett. **51**, 308 (1983).
[17] C. Rossel *et al.,* Phys. Rev. B **35**, 1914 (1987).
[18] Z. Fisk and M. B. Maple, J. Alloys Compd. **183**, 303 (1992).